

NANOSCALE TOUGHENING MECHANISMS OF ULTRA HIGH TEMPERATURE  
NOVEL HfB<sub>2</sub> BASED MULTIPHASE CERAMICS

by

ZOHER SHABBIR LAVANGIA

Presented to the Faculty of the Graduate School of  
The University of Texas at Arlington in Partial Fulfillment  
of the Requirements  
for the Degree of

MASTER OF SCIENCE IN AEROSPACE ENGINEERING

THE UNIVERSITY OF TEXAS AT ARLINGTON

May 2015

Copyright © by Zoher Shabbir Lavangia 2015

All Rights Reserved



### Acknowledgements

It would not be possible to name every individual who have contributed towards the completion of my thesis and throughout the Master's course. I would start by thanking my advisor, Dr. Adnan Ashfaq for giving me the opportunity to explore a completely different field than previously undertaken, and to have helped immensely in achieving my goals. I also thank Dr. Kent Lawrence and Dr. Wen Chan for serving on my defense committee.

Furthermore, without the efforts of my senior, Sheikh Ferdous Fahad it would not be possible to have completed this thesis. His guidance has allowed me to come up to speed with Molecular Dynamics Simulations and processing techniques.

I would also take this opportunity to thank my parents Fatema and Shabbir Lavangia, my sister Jameela Sabir and fiancé, Jameela Rupawala for their continued support and encouragement without which this would have not been possible. I am also grateful to my friends for their love and support.

April 15, 2015

## Abstract

### NANOSCALE TOUGHENING MECHANISMS OF ULTRA HIGH TEMPERATURE

#### NOVEL HfB<sub>2</sub> BASED MULTIPHASE CERAMICS

Zoher Shabbir Lavangia, MS

The University of Texas at Arlington, 2015

Supervising Professor: Adnan Ashfaq

During return of spacecraft they endure very high temperatures (3000°F), few materials can withstand temperatures this high along with additional loads of the spacecraft. Reinforced carbon-carbon (RCC) material system is used as Thermal Protection System (TPS) which is made of laminated graphite rayon-phenolic epoxy, which need to sustain extreme heat. However, these materials are very prone to premature degradation due to oxidation. Silicon Carbide (SiC) and Hafnium Diboride (HfB<sub>2</sub>) are candidate materials for TPS but, they inherently lack the required toughness for such applications. This research is carried out in two stages, first is to study the individual properties of SiC and HfB<sub>2</sub> at high temperatures and different crack lengths at the center, second is to combine the two materials in a layered structure and evaluate the properties thus changed due to their composite form. The study is carried out using Molecular Dynamics Simulation (MDS) techniques and a considerable improvement in the tensile strength of the Nano-composite is found.

This study investigates Silicon Carbide (SiC) and Hafnium Diboride (HfB<sub>2</sub>) Nano-composites layers as an alternative to RCC. Behavior of these materials have been studied using Molecular Dynamics Simulation (MDS). As individual materials they are susceptible to low toughness, but study shows that their Nano-composite form in suggested configurations can improve their toughness characteristics and retain it at high temperatures making them suitable for TPS.

## Table of Contents

Acknowledgements .....	iii
Abstract .....	iv
List of Illustrations .....	vii
List of Tables .....	ix
Chapter 1 Structural Technologies .....	1
Chapter 2 Molecular Dynamics Simulation Background.....	4
Introduction to DL_POLY .....	7
Units.....	7
Force Field Algorithms.....	8
Tersoff Potential Function (covalent potential) .....	9
Compiling the Simulations .....	10
CONFIG file .....	11
FIELD file .....	11
CONTROL file.....	12
REVCON file.....	12
STATIS file.....	12
Test Procedure and Conditions: .....	13
Post Processing MDS Output.....	14
Stress Calculation.....	14
Fracture toughness.....	14
Chapter 3 Fracture Behavior of Silicon Carbide (SiC) Nano-Film .....	17
Overview .....	17
Crystal Structure .....	17
Silicon Carbide models for Molecular Dynamics Simulation .....	19

Results and Discussions .....	22
Effect of Thickness on Elastic Properties of SiC Nano-film.....	22
Effect of Temperature on Behavior of SiC Nano-film .....	23
Chapter 4 Fracture Behavior of Hafnium Diboride (HfB <sub>2</sub> ) Nano-Film .....	27
Overview .....	27
HfB <sub>2</sub> Simulation Models: .....	29
Results .....	30
Effect of Temperature on Behavior of HfB <sub>2</sub> .....	30
Chapter 5 Fracture Behavior of Layered Multi-Phase Composite Nano-Film .....	33
Results .....	35
Multiphase Properties of Layered Nano-Film .....	35
Effect of Temperature on Behavior of Layered HfB <sub>2</sub> -SiC Nano-film .....	37
Chapter 6 Conclusion.....	40
Bibliography .....	44
Biographical Information .....	47

## List of Illustrations

Figure 1-1 Comparison of thermal conductivity for high temperature materials (Johnson, August 3, 2011).....	2
Figure 2-1 Schematic of MDS execution procedure. ....	6
Figure 2-2 Input and output files for DL_POLY.....	10
Figure 2-3 Schematic of Simulation model and procedure.....	13
Figure 2-4 Total energy plot w/ time for SiC w/ center crack 3a. ....	16
Figure 3-1 (a) 3C-SiC crystal (Miriam López-Álvarez, 2011); (b) Stacking sequence of SiC polytypes. ....	18
Figure 3-2 SiC model using DL_POLY GUI.....	19
Figure 3-3 Centre crack models with length (i) 13.08Å; (ii) 17.44Å; (iii) 21.79Å .....	20
Figure 3-4 Illustration of the crack propagation and failure for SiC with center crack length = 13.08Å .....	20
Figure 3-5 Plot showing Young's modulus of SiC vs. Thickness in z-direction. ....	22
Figure 3-6 Plot showing Poisson's ratio of SiC vs. Thickness in z-direction. ....	23
Figure 3-7 Plot of Stress vs. Strain for SiC w/ center crack = 3a.....	25
Figure 3-8 Plot of Stress vs. Strain for SiC w/ center crack = 4a.....	26
Figure 4-1 HfB <sub>2</sub> crystal structure. (Wataru Hayami, 1998).....	27
Figure 4-2 HfB <sub>2</sub> model using DL_POLY GUI. ....	29
Figure 4-3 Plot of Stress vs. Strain for HfB <sub>2</sub> w/ center crack = 2a. ....	31
Figure 4-4 Plot of Stress vs. Strain for HfB <sub>2</sub> w/ center crack = 3a. ....	32
Figure 5-1 Layered nano-film model. ....	34
Figure 5-2 Phase Diagram of Hf - B.....	35
Figure 5-3 Phase diagram for Si - C .....	36
Figure 5-4 Energy vs. Temperature plot for Layered Nano-film. ....	37

Figure 5-5 Plot of Stress vs. Strain for HfB <sub>2</sub> - SiC w/ center crack = 3a. ....	39
Figure 6-1 Comparison of Layered HfB <sub>2</sub> -SiC tensile strength to individual elements. ....	40
Figure 6-2 Comparison of Layered HfB <sub>2</sub> -SiC toughness to individual elements.....	41
Figure 6-3 Illustration of layered HfB <sub>2</sub> -SiC failure. ....	42
Figure 6-4 Suggested improvements at the interface to further improve toughness.....	42



## List of Tables

Table 3-1 SiC material properties (G.F. Dirras a, 2004).....	18
Table 3-2 SiC material properties -2.....	19
Table 3-3 Tersoff potential data for Si and C atoms (S Satake, 2009) .....	21
Table 3-4 SiC properties derived after Post-processing MDS data. ....	24
Table 4-1 Properties of HfB <sub>2</sub> .....	28
Table 4-2 Tersoff potential data for Hf and B atoms (Murray S. Dawa, 2011). ....	28
Table 4-3 HfB <sub>2</sub> properties derived after Post-processing MDS data. ....	30
Table 5-1 Layered HfB <sub>2</sub> -SiC properties derived after Post-processing MDS data. ....	38
Table 6-1 Tensile strength improvement in layered HfB <sub>2</sub> -SiC .....	41

## Chapter 1

### Structural Technologies

With the advancement in technology today there is an increasing need of products with a high reliability factor. At the core of any structure whether it is of the size of a penny or it is a structure as big as the largest passenger aircraft, structural design is one of the most essential factors in the development process. Some structures require materials to undergo large temperature variations during operation. Temperature variations could be in the range of a few degrees in case of hand held smartphones and other mobile devices but could be as high as 3000°F in case of space shuttle re-entry to the earth's atmosphere. In both cases, it is essential for the material to operate reliably over and over again for maximizing operating life. But there are very few materials present in nature which can provide such high usability and reliability for high temperature applications. The most common of these are widely known as ceramics. Although ceramics are great for applications involving high temperatures, they are susceptible to failure without any warning and possess comparatively lower strength. It is also essential for structures to be light weight to increase efficiency, reduce costs and for aesthetics in case of consumer products.

Thus, to improve the behavior of materials to withstand high thermal loads and ensure reliable operation there is a necessity to develop novel materials specific to such applications. Studying about their fracture behavior gives more insight into its behavior under operating conditions. This study explores novel Hafnium Diboride (HfB<sub>2</sub>) based multi-phase ceramics as alternative ultra-high temperature materials towards aerospace applications in hypersonic and re-entry vehicles. Silicon Carbide (SiC) is used as a layered structure with HfB<sub>2</sub> to increase toughness. This will be applied as nano-coatings to structures that endure high temperatures to enhance fracture toughness

These studies are carried out using DLPOLY\_2.20 (I.T. Todorov, 2006) to carry out Molecular Dynamics Simulations (MDS) which will be discussed in further chapters. Temperature from 300 k to 2100 K are tested to measure the characteristics of this material system. Analysis of pure SiC and HfB<sub>2</sub> are carried out and compared to layered configurations and conclusions are drawn based on the results thus obtained.

#### Why Hafnium Diboride and Silicon Carbide?

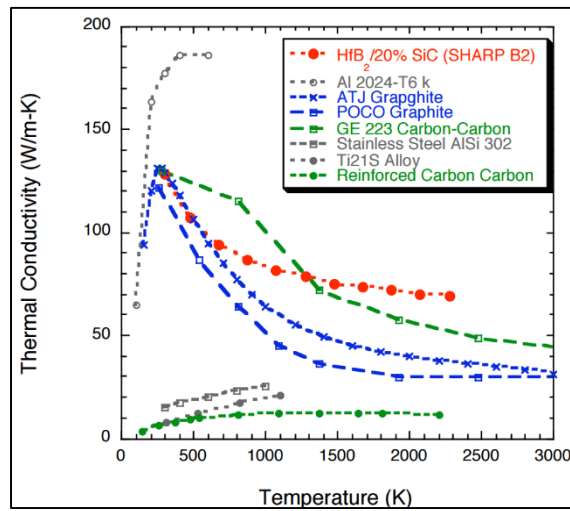


Figure 1-1 Comparison of thermal conductivity for high temperature materials (Johnson, August 3, 2011).

Extensive studies have been carried out on Zirconium Diboride (ZrB<sub>2</sub>) and Hafnium Diboride (HfB<sub>2</sub>) as potential Ultra-High Temperature Ceramic Materials (UTHC) in the past (M.J. Thompson, November 30, 2011) (J. Marschall, 2011) (. J. Watts, 2011). The dispersion of nano-particles to improve fracture toughness within the material plays a significant role (Ferdous, 2012) (Sheikh F Ferdous M. F., 2013). Figure 1-1 shows the thermal conductivity of HfB<sub>2</sub>-SiC system is superior to other high temperature alloys and composites (John W. Lawson). Thermal Protection systems for re-entry vehicles and leading edges of hypersonic vehicles operate under extreme conditions and are in contact

with oxygen present in the atmosphere. Oxidation occurs at high temperatures and results in loss of electrons from the material which decreases the physical characteristics of the material (Duffy, April 1999). Studies have shown good oxidation properties for SiC Nanoparticles in HfB<sub>2</sub> (Xinghong Zhang, 15 August 2008).

## Chapter 2

### Molecular Dynamics Simulation Background

Computer simulations play a very crucial role in engineering technology today (Iazar, 2005). In the past, data was analyzed manually and was largely simplified under ideal world assumptions. The same was with experimental data which lacked the real world complexities in its testing equipment because it is costly as well as time consuming to simulate real world scenarios with physical experiments. Furthermore, it was not possible to test all conditions described in theory and models had to be simplistic. In reality most of the interesting physical problems are beyond the simple cases and would not give any clear idea of what the results might indicate.

With the advancement in computational power, it was made possible to model the previously simplified cases in to more realistic data and obtain results. Over time the speed of computational power has changed significantly. Problems that would take weeks to solve can now be computed in a matter of seconds. Also with time the reliability of results obtained has increased.

Molecular dynamics simulation process is realized by the numerical, step-by-step, solution of the classical Newton's equations of motion (Basics of Molecular Dynamics):

$$\begin{aligned} m_i \ddot{r}_i &= f_i; \\ f_i &= -\frac{\partial U_i(r^n)}{\partial r_i} \end{aligned} \quad 2.2-a$$

Where  $m_i$  represents the mass of the particle 'i', in most case an atom;  $f_i$  represents the force on i and  $r_i$  represents the position vector. In most cases the forces are derived from the potential functions,  $U(r_1, r_2, \dots, r_n)$ , representing the potential energy of the system for the specific arrangement. In the absence of external forces, the sum of pairwise interactions can pose as a representation to the potential. When considering temperature  $T$  and the density  $\rho$  as independent variables, the energy  $E$  and pressure  $P$

can be readily expressed in molecular dynamics simulations and is a link between the microscopic and the macroscopic level.

Certainly the behavior of finite systems (Nano level) is very different from infinite systems (continuum level). Irrespective of the number of molecules considered in defining the system geometry its scale will be negligible to that of a system designed at macroscopic level. To overcome surface interaction effects for a large simulation it is effective to use periodic boundary condition. Periodic boundary condition implies that particles are enclosed in a box, replicating rigid translation up to infinity in the three Cartesian co-ordinate. After each integration co-ordinates of the particles are examined and readjusted to bring it back to the boundary. For the purpose of this study all molecular dynamic simulations are carried out using DL\_POLY\_2.20.

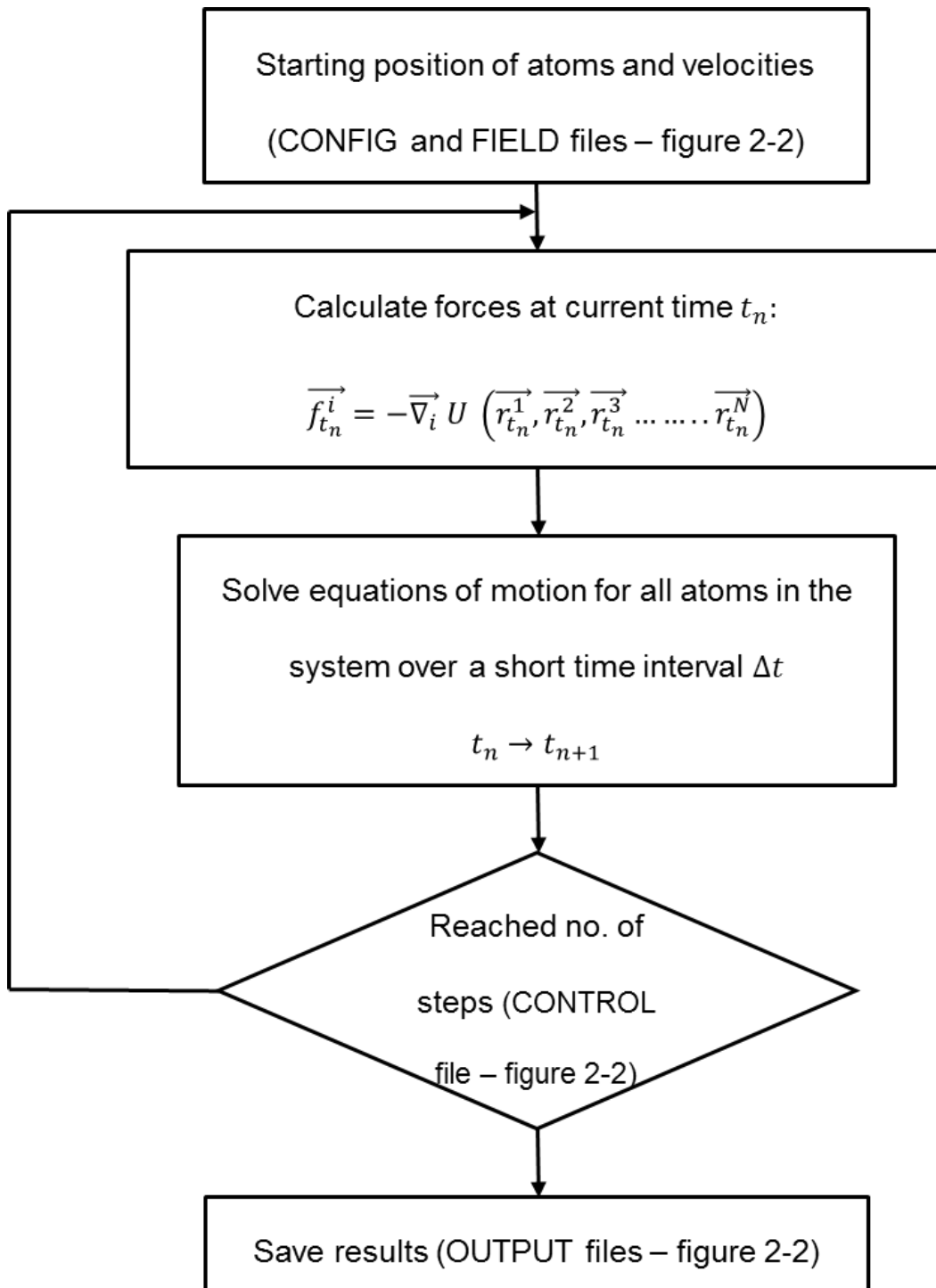


Figure 2-1 Schematic of MDS execution procedure.

## Introduction to DL\_POLY

DL\_POLY is a package written exclusively in FORTRAN 90 (W. Smith, 2009) and consist of subroutines, programs and data files that allow molecular dynamics simulations of macromolecules, polymers, ionic systems and other molecular systems on a distributed memory parallel computer. This package is written by Bill Smith and Tim Foster under grants from Engineering and Physical Sciences Research Council and is the property of the Science and Technology Facilities Council. The DL\_POLY\_2.20 version is capable of simulating 30,000 atoms on up to 100 processors and can support many molecular species like simple atomic systems and mixtures, polarizable and un-polarizable point ions, rigid molecules, polymers, metals, covalent systems and many more.

### Units

All DL\_POLY\_2.20 subroutines and functions assume the following defined molecular units (W. Smith, 2009):

- i. Time ( $t_0$ ) – picoseconds ( $= 1 \times 10^{-12}$  seconds)
- ii. Length ( $l_0$ ) – Angstrom ( $= 1 \times 10^{-10}$  meters)
- iii. Mass ( $m_0$ ) – atomic mass units ( $= 1.6605402 \times 10^{-27}$  kilograms)
- iv. Charge ( $q_0$ ) – unit of proton charge ( $1.60217733 \times 10^{-19}$  coulombs)
- v. Energy ( $E_0 = m_0(l_0/t_0)^2$ ) –  $1.6605402 \times 10^{-23}$  Joules
- vi. Pressure ( $P_0 = E_0 l_0^{-3}$ ) –  $1.6605402 \times 10^7$  Pascal
- vii. Temperature – Kelvin



## Force Field Algorithms

These are a set of functions that define molecular interactions for a given system. DL\_POLY allows the user to define these parameters for the system or can use other resources to generate data.

DL\_POLY defines total configuration energy as;

$$U(r_1, r_2, \dots, r_N) = \sum U_{bond} + \sum U_{angle} + \sum U_{dished} + \sum U_{inv} + \sum U_{pair} + \sum U_{3\ body} + \sum U_{Tersoff} + \sum U_{4\ body} + \sum U_{Metal} + \sum U_{extn} \quad 2-2-b$$

Where,  $U_{bond}$ ,  $U_{angle}$ ,  $U_{dished}$ ,  $U_{inv}$ ,  $U_{pair}$ ,  $U_{3\ body}$ ,  $U_{Tersoff}$  and  $U_{4\ body}$  are empirical functions representing Chemical bonds, valance angles, dihedral angles, inversion angles, pair-bonds, three-body, Tersoff and four-body forces respectively.  $U_{Metal}$  and  $U_{extn}$  are metal and external field potentials respectively.

The calculation of bonded forces therefore follows the simple scheme:

- i. Each atom is assigned a unique identification number by its index starting from 1
- ii. Each intra-molecular term having a 'Utype' bond in the system has a unique index number 'itype' from 1 to 'Ntype' wherein the 'type' can be either bond, angle or dihedral.
- iii. 'keytype' is an array pointer (ntype, itype) which includes indices of the specific atoms taking part in the potential defined by 'itype'. 'ntype' has a dimension of 2, 3 or 4, to indicate a bond, valance angle or dihedral /inversion.
- iv. Now 'keytype' will be used as an identifier for atoms within a bonded term to assign right interactions in calculating energy and forces.

### Tersoff Potential Function (covalent potential)

In this study we make use of Tersoff potential and so we will discuss about it in detail here. The Tersoff potential can be classified as a density dependent potential, specially designed to replicate of covalent bonding properties in system containing carbon, silicon, germanium etc. and alloys of these elements. This potential offers bond breaking and bond hybridization as special feature and has 11 atomic and 2 bi-atomic parameters.

It is of the following form;

$$U_{ij} = f_C(r_{ij})[f_R(r_{ij}) - \gamma_{ij}f_A(r_{ij})], \quad 2-2-c$$

where,

$$f_R(r_{ij}) = A_{ij} \exp(-a_{ij}r_{ij}); f_A(r_{ij}) = B_{ij} \exp(-b_{ij}r_{ij}) \quad 2-2-d$$

$$f_C(r_{ij}) = \begin{cases} 1 & : r_{ij} < R_{ij} \\ \frac{1}{2} + \frac{1}{2} \cos[\pi(r_{ij} - R_{ij})/(r_{ij} - R_{ij})] & : R_{ij} < r_{ij} < S_{ij} \\ 0 & : r_{ij} > S_{ij} \end{cases} \quad 2-2-e$$

$$\gamma_{ij} = \chi_{ij} (1 + \beta_{ij} \mathcal{L}_{ij})^{-\frac{1}{2}\eta_i}, \mathcal{L}_{ij} = \sum_{k \neq i, j} f_C(r_{ik}) \omega_{ij} g(\theta_{ijk}) \quad 2-2-f$$

Here,  $i, j$  and  $k$  denote the atoms in the simulation,  $r_{ij}$  is the length of the bond and  $\theta_{ijk}$  is the angle between bonds  $ij$  and  $ik$ . In the absence of a second script it denotes that the value is unique to that atom type.  $\chi_{ij}$  and  $\omega_{ij}$  are bi-atomic parameters that define the interactions between different atom types.

Tersoff potentials are short ranged to the order of 3 Å and its two and three body contributions scale as  $N^3$ , where  $N$  is the number of particles. This is important for link-cell method.

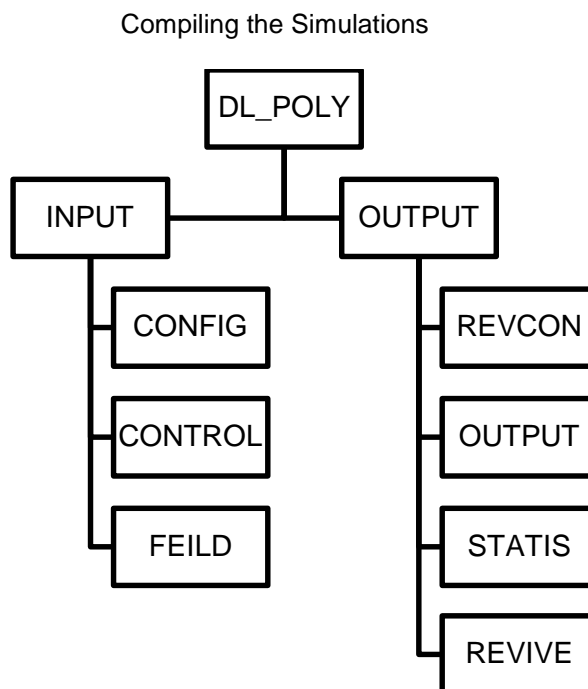


Figure 2-2 Input and output files for DL\_POLY.

To run any simulation you require the files CONTROL, FIELD and CONFIG after execution the program will generate the files OUTPUT, REVCON and REVIVE, also based on your options before executing the program can also generate the files STATIS, HISTORY, RDFDAT and ZDNDAT.

Executing procedure in DL\_POLY (W. Smith, 2009):

- i. Compile three essential input files for running in DL\_POLY. First of which is CONFIG, this files contains all the data regarding the configuration of the molecular system. The second input file is Field, this file determines the interactions parameters for the molecular system defined in the CONFIG file. The third file, CONTROL is the set of instructions for DL\_POLY i.e. it directs the program to run with certain conditions set for

the molecular system. For the very first simulation the molecular system is only equilibrated.

- ii. After execution DL\_POLY returns the OUTPUT, REVCN, REVIVE and STATIS. The OUTPUT file contains the summary of simulation results, instantaneous averaged data, input data, job time etc. The REVIVE file is not readable, but contains information regarding the job run for use as the input file in the next run. REVCN contains the final position, velocities and forces of the atoms at the end of the run. The STATIS file contains the instantaneous values of all variables in the simulation and is used for post processing.
- iii. The next step after equilibration is to perform tensile (shear/compression) tests based on the data required. For the purpose of this simulation the output files from the equilibration stage will be retained. The CONTROL file will be modified to run in loop for such tests. The REVCN will be used as the CONFIG file and similarly REVIVE will be USED as REVOLD. The FIELD file is retained as is. After running the required tests the data from the STATIS file can be imported into EXCEL for further analysis.

#### CONFIG file

This file contains the dimensions of the unit cell (W. Smith, 2009), the essential periodic conditions and atomic label, co-ordinates, velocity and forces. For this research the CONFIG files were created using the DL\_POLY Graphical User Interface (GUI).

#### FIELD file

This file contains information regarding the interaction of molecules (W. Smith, 2009) in the system. This is achieved via the potential function parameters. In order

to define these parameter it is important to have the molecule information arranged in sync with the CONFIG file.

#### CONTROL file

As the name suggests this file pertains to the necessary control parameters to execute the simulation. It defines the temperature (W. Smith, 2009) of the molecular simulation, the number of steps that it will perform, the cut-off forces etc. This file contains the command to start execution of a new type or to continue from a previous round of simulation.

#### REVCON file

After the program is executed DL\_POLY generates file OUTPUT, REVIVE, REVCON and STATIS. We will discuss REVCON and STATIS since they will be used for post processing and simulation result visualization.

A REVCON file is essentially similar to a CONFIG file but contains the atomic configuration of the system on completion of the simulation (W. Smith, 2009). If the program is restarted the REVCON filename must be changed to CONFIG. This file can be viewed in the DL\_POLY GUI to visualize the results of the final configuration.

#### STATIS file

This file contains the numerical data recorded for the molecular system at the intervals specified in the CONTROL file. The energy unit is as specified in the CONTROL file and remaining data is compatible with data appearing in the OUTPUT file. The values are assigned in the form an array, each value denotes a statistical value of the system. The last 9 values in the array represent the stress tensor. Using FORTRAN codes, these values are extracted and averaged in a separate file which is then imported to EXCEL for post processing and analysis.

### Test Procedure and Conditions:

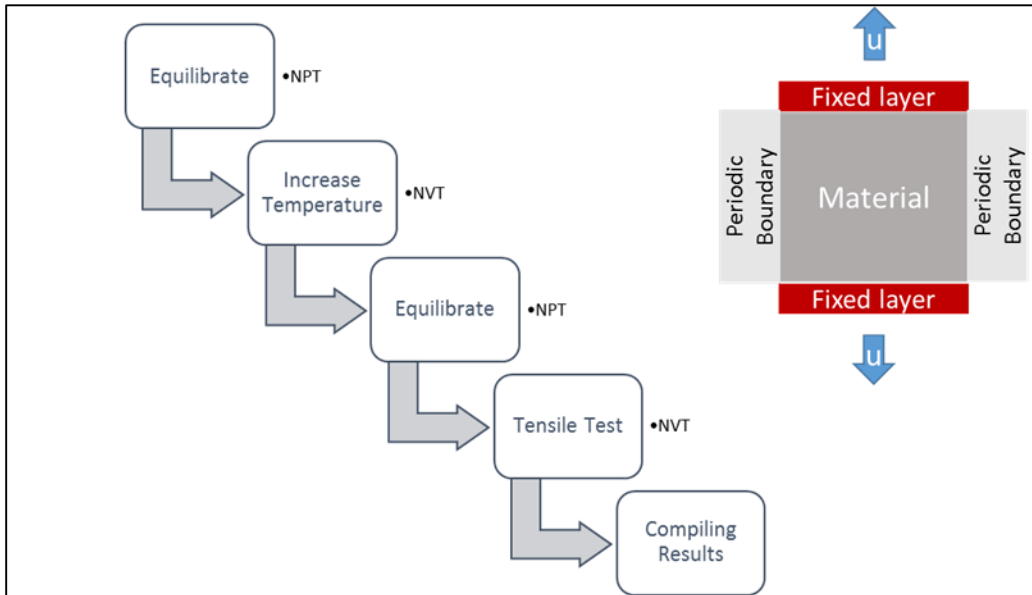


Figure 2-3 Schematic of Simulation model and procedure.

Figure 2-3 shows the steps carried out while simulating in DL\_POLY and a representation of material geometry with boundary conditions to carry out tensile tests. All simulations will be carried out from 300 K- 1800 K with a step of 500 K to study the effects of Temperature. At the beginning each model is equilibrated using canonical ensemble, NPT (Spearot, August 2005) conditions which is essentially maintaining the number of atoms, pressure and temperature constant. The temperature of the systems is increased in steps of 20 K and equilibrated at every 2000 steps, this is done to avoid large fluctuations in energy and thus obtain a stable system. After Equilibrium the models will be subjected to a tensile/shear loading in the form of constant displacement at the “fixed” layers. After each increment in displacement the system will equilibrate for 2000 steps and the next 1000 steps will generate average the sample data values. We will use the isobaric-isothermal ensemble, NVT which keeps the number of atoms, volume and temperature constant during the tensile test.

## Post Processing MDS Output

### *Stress Calculation*

At atomistic level the Stress component ( $\sigma_{ij}$ ) is represented by the virial stress (Arun K. Subramaniyan, July 2008), which is given by;

$$\sigma_{ij} = -\frac{1}{V} \sum_{\alpha} \left( M^{\alpha} v_i^{\alpha} v_j^{\alpha} + \frac{1}{2} \sum F_j^{\alpha\beta} r_j^{\alpha\beta} \right) \quad 2-g$$

where, 'i' 'j' are directions x and y respectively,

$\beta$  - varies from 1 – N neighbors of atom  $\alpha$ ,

$\alpha$  – position of atom  $\alpha$  along i-direction,

$F_j^{\alpha\beta}$  - is the force on atom  $\alpha$  in j-direction due to atom  $\beta$

V – Total Volume,

$M^{\alpha}$  – is the mass of atom  $\alpha$

These values are extracted from STATIS file using a FORTRAN code and converted to an EXCEL data. This can then be plotted as Stress vs. Strain curve.

### *Fracture toughness*

Fracture toughness is a quantitative way of defining a material's ability to resist failure in the presence of crack (Microtek Laboratories). It indicates the amount of stress that will be required to propagate any existing flaw in the material. During the 1920's Griffith formulated a theory predominantly for brittle materials that stated that, if the change in elastic strain energy due to the presence of crack is greater than the energy required to create new crack surfaces, the result will be propagation of that crack. (Julie A. Bannantine, 1989). There are three types of fracture modes depending on the type of loading and its direction, they are; (1) Mode I – opening or Tensile mode, (2) Mode II – Sliding or in plane

shear mode, (3) Mode III – tearing or anti-plane shear mode (Roylance, Introduction to Fracture Mechanics, 2001). This study is only focused on Mode I failure.

'G' is called as the energy per unit area of crack or critical strain energy release rate at fracture initiation;

$$G = \frac{\partial U}{B \times \partial a}; K_{IC} = \sqrt{\left(\frac{E \times G}{1 - \nu}\right)} \quad 2-h$$

where;  $\partial U$  – energy gradient between two cracksize

$\partial a$  – difference in crack length

B – thickness

$K_{IC}$  – stress intensity fracture for mode one fracture

To calculate the energy difference to form new surface in presence of crack, the corresponding STATIS file is evaluated in the DL\_POLY GUI. This generates a plot of Energy vs. Time as shown in figure 2-4. Once the system reaches equilibrium the energy value remains constant which is used for further assesment.



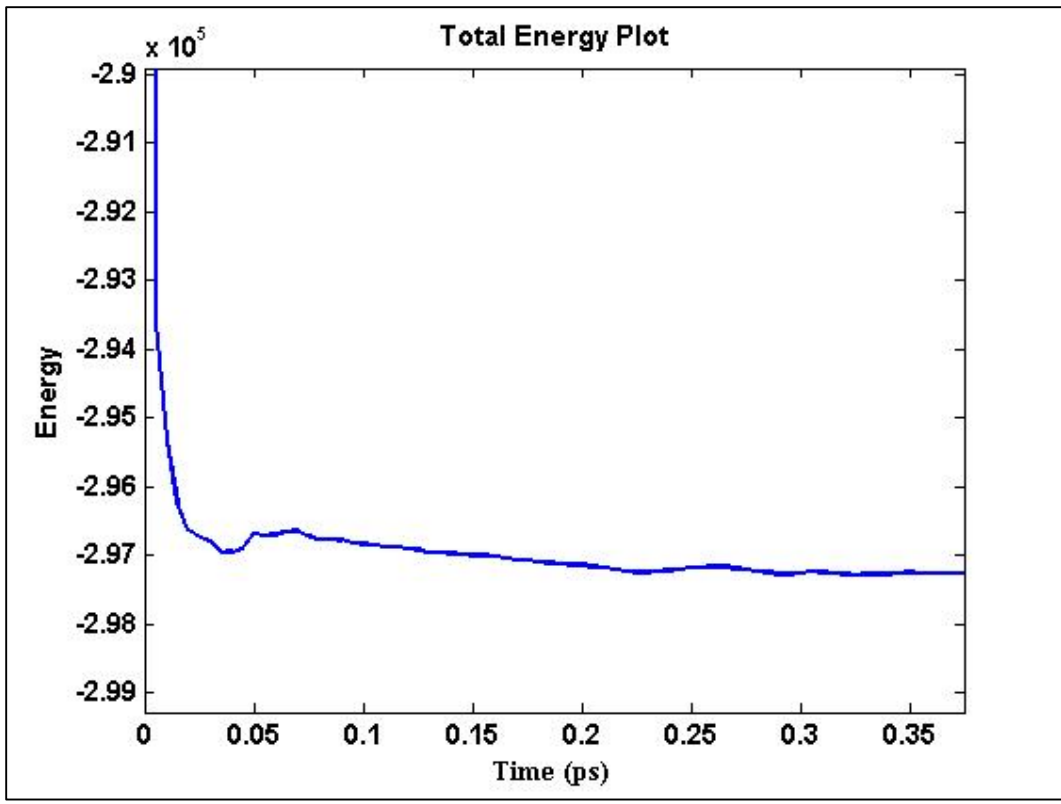


Figure 2-4 Total energy plot w/ time for SiC w/ center crack 3a.

## Chapter 3

### Fracture Behavior of Silicon Carbide (SiC) Nano-Film

#### Overview

Silicon Carbide (SiC) is a well-known ceramic material with practical properties like high thermal conductivity, mechanical strength, chemical inertness (Ashfaq Adnan, January 2015) and the ability to operate at high temperatures is often used in various applications ranging from electronic devices, refractory materials, brake pads aerospace components etc. The recent advances in processing techniques of SiC has encouraged its use in thin film SiC optics, opto-electronics, micro-machining, MEMS (G.F. Dirras a, 2004), etc. Studies of SiC with diamond nano-particles have shown positive results (Sheikh F Ferdous, 2013). The behavior of thin films is essential for applications in the semiconductor and the aerospace industry, the results for fracture toughness using molecular dynamics approach is reported in this thesis will enhance the understanding of them.

#### Crystal Structure

Silicon Carbide is covalently bonded semiconductor, with each silicon having a covalent bond with four carbon atoms resulting in a tetrahedron (Fan & Chu, 2014). Tetrahedron's are represented by two types and double-atomic layers by three types named 'A', 'B' and 'C' which form a periodic series along the c-axis with a specific pattern representing a polytype as shown in figure 3-1-b. The 3C-SiC shown in figure 3-1-a is the only cubic structured Silicon Carbide polytype and will be studied for this study, the C represents the cubic nature and 3 refers to the number of double-atomic layers.

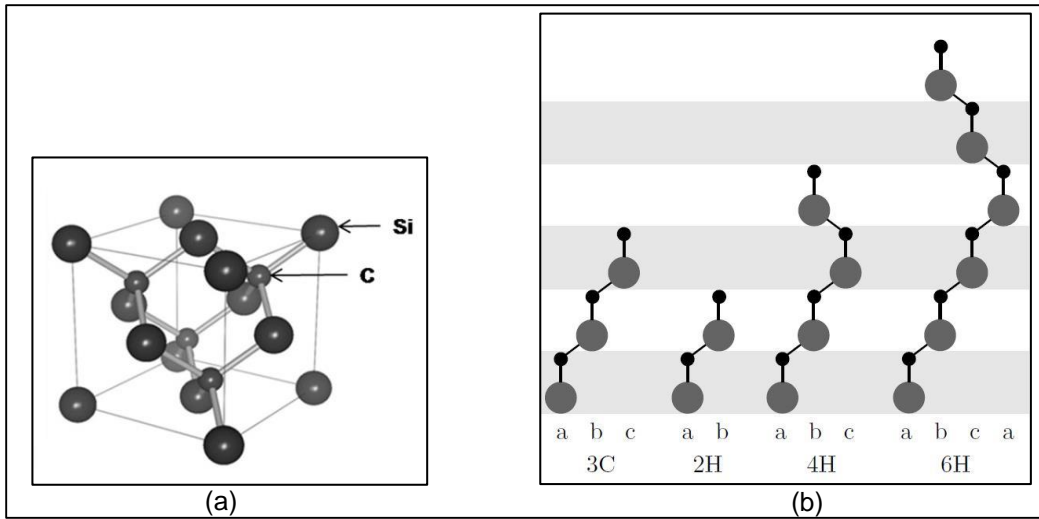


Figure 3-1 (a) 3C-SiC crystal (Miriam López-Álvarez, 2011); (b) Stacking sequence of SiC polytypes.

Table 3-1 SiC material properties (G.F. Dirras a, 2004)

Single crystal	Poly-crystal
c11 (GPa) $395 \pm 12$	C11 $500 \pm 30$
-	C33 $535 \pm 10$
c44 (GPa) $236 \pm 7$	C44 $165 \pm 10$
-	C66 $210 \pm 10$
c12 (GPa) $132 \pm 9$	C13 50

Table 3-2 SiC material properties -2

	Single crystal $\beta$ -SiC	Polycrystalline $\beta$ -SiC
Young's modulus, E (GPa)	$420 \pm 50$	$430 \pm 40$
Poisson's ratio, $\nu$	0.19	0.24

### Silicon Carbide models for Molecular Dynamics Simulation

Using the DL\_POLY GUI different models are prepared to simulate tensile test and obtain properties for SiC. The model shown in figure 3-2 contains 75,000 Si and C atoms as part of the main material and 6,000 Al and N atoms as part of the layer at the top and bottom of SiC structure. This additional layer will be fixed (interactions between these atoms are not calculated) and will be used to apply displacement boundary condition during tensile test (figure 2-3).

Lattice constant,  $(a) = 4.3589 \text{ \AA}$ ;

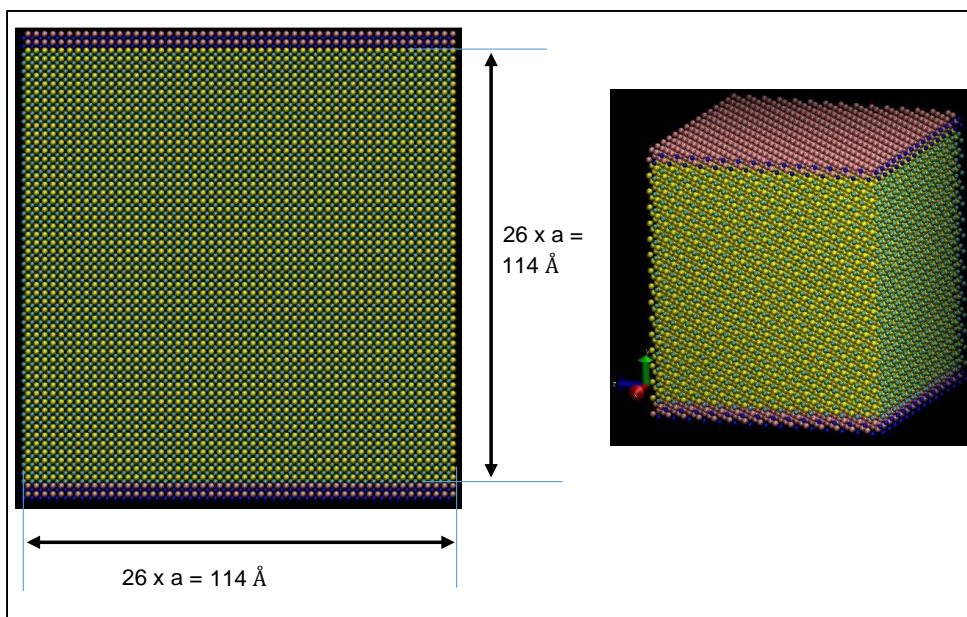


Figure 3-2 SiC model using DL\_POLY GUI.

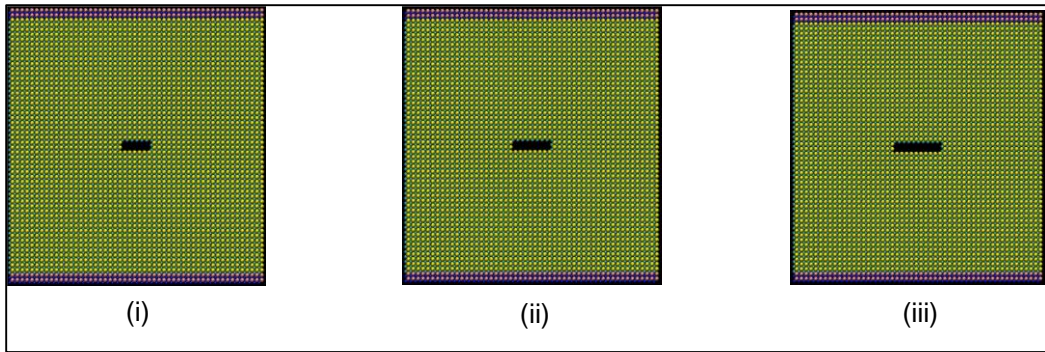


Figure 3-3 Centre crack models with length (i) 13.08Å; (ii) 17.44Å; (iii) 21.79Å

Figure 3-3 shows the different crack lengths that will be studied to find the fracture toughness of the material as discussed earlier. Figure 3-4 shows the behavior of SiC under tensile test. As predicted for brittle failure, SiC does not show any necking during failure and follows a clean and straight propagation of crack.

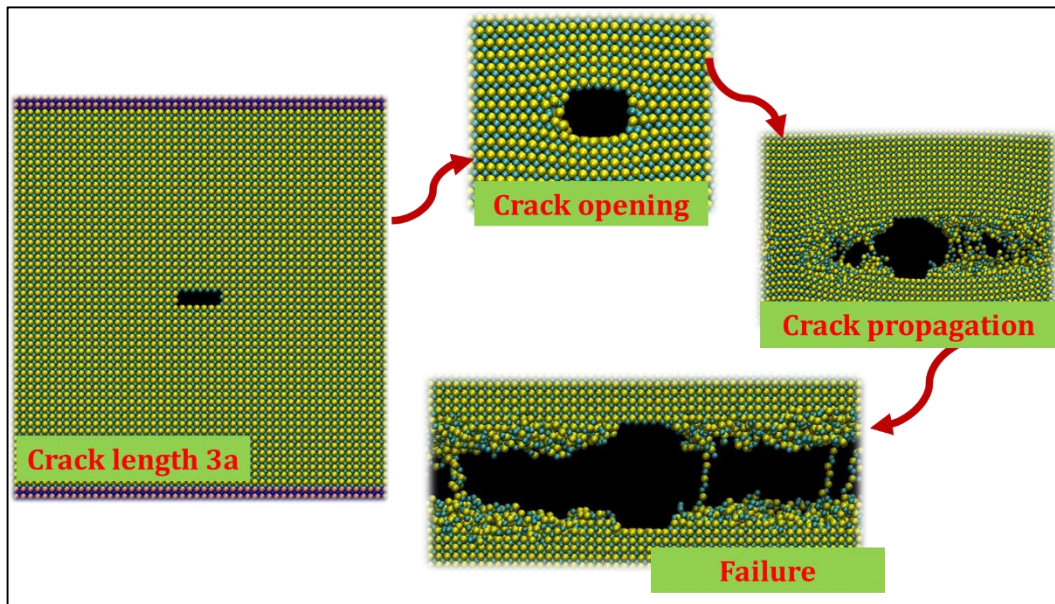


Figure 3-4 Illustration of the crack propagation and failure for SiC with center crack length = 13.08Å

Table 3-3 Tersoff potential data for Si and C atoms (S Satake, 2009)

<b>Parameter</b>	<b>C</b>	<b>Si</b>
A [eV]	1.3936x10 <sup>3</sup>	1.83x10 <sup>3</sup>
B [eV]	3.467x10 <sup>2</sup>	4.7118x10 <sup>2</sup>
$\lambda$ [Å <sup>-1</sup> ]	3.4879	2.4799
$\mu$ [Å <sup>-1</sup> ]	2.2119	1.7322
$\beta$	1.5724x10 <sup>-7</sup>	1.10x10 <sup>-5</sup>
$\eta$	7.2751x10 <sup>-1</sup>	7.8734x10 <sup>-1</sup>
c	3.8049x10 <sup>4</sup>	1.0039x10 <sup>5</sup>
d	4.384	16.217
h	-0.57058	-0.59825
R (1) [Å]	1.8	2.7
R (2) [Å]	2.1	3

<b>Combination</b>	<b><math>\epsilon</math> [eV]</b>	<b><math>\sigma</math> [Å]</b>
Si-C	2.461	3.555

The Tersoff potential parameters in the above table are a representation of the force field algorithms discussed in the previous chapter (2) and is used as input in the FIELD file which governs the interaction of atoms within the system.

## Results and Discussions

### *Effect of Thickness on Elastic Properties of SiC Nano-film*

It is necessary to be sure of the accuracy given by the output of any simulation that we run so that the data can be reliable. For this reason a series of tensile tests were carried out and elastic properties calculated with the variation of thickness from 4.36Å-39.23Å with an increment of 4.36Å (SiC lattice constant) along the z-direction for the SiC crystal.

The results for Young's modulus and Poisson's ratio are plotted against thickness and shown in figure 3-5 and 3-6.

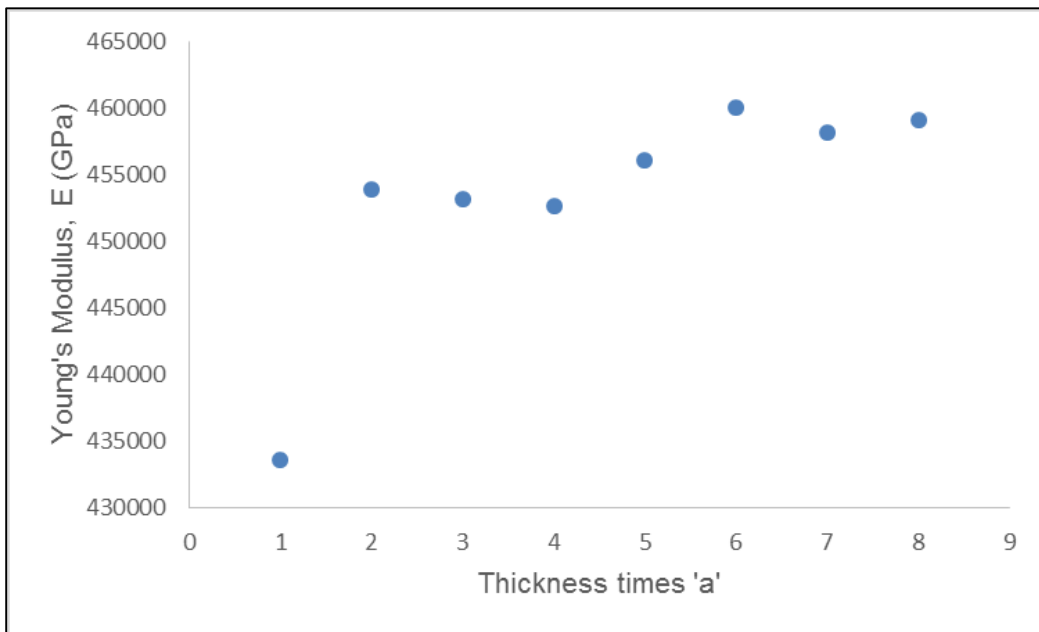


Figure 3-5 Plot showing Young's modulus of SiC vs. Thickness in z-direction.

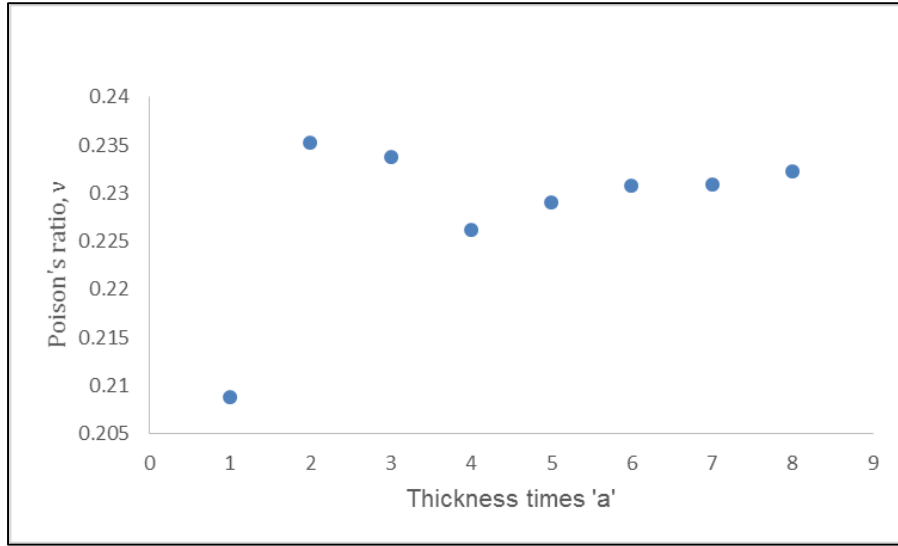


Figure 3-6 Plot showing Poisson's ratio of SiC vs. Thickness in z-direction.

The plots clearly indicate poor results for very low thickness but show a consistent trend for thickness greater than 5 times the lattice constant i.e. 20 Å.

#### *Effect of Temperature on Behavior of SiC Nano-film*

After establishing confidence in the results obtained from these simulations, tensile tests on the various models of SiC were executed with periodic boundary conditions and a displacement of 0.05.

We know the linear relation of Stress vs. Strain can be represented in the form;

$$\epsilon_{ij} = S_{ijkl} \sigma_{kl} \quad 3-a$$

$$\begin{Bmatrix} \epsilon_x \\ \epsilon_y \\ \epsilon_z \\ \gamma_{yz} \\ \gamma_{xz} \\ \gamma_{xy} \end{Bmatrix} = \begin{bmatrix} S_{11} & S_{12} & \cdots & S_{16} \\ S_{21} & S_{22} & \cdots & S_{26} \\ \vdots & \vdots & \ddots & \vdots \\ S_{61} & S_{26} & \cdots & S_{66} \end{bmatrix} \begin{Bmatrix} \sigma_x \\ \sigma_y \\ \sigma_z \\ \tau_{yz} \\ \tau_{xz} \\ \tau_{xy} \end{Bmatrix} \quad 3-b$$

Where, S is called the compliance matrix (Roylance, Laminated Composite Plates, 2000). If 'ijkl' are considered as separate indices the S matrix will have 81 independent



components. However as we see in eq<sup>n</sup> 4-b,  $\varepsilon$  and  $\sigma$  are symmetric which results in reducing the compliance matrix components to 36. Further simplification to an isotropic material can reduce the number of independent elements in the compliance matrix to 2. They are;

$$\varepsilon_x = \frac{1}{E} (\sigma_x - \nu \sigma_y) \quad 3-c$$

$$\varepsilon_y = \frac{1}{E} (\sigma_y - \nu \sigma_x) \quad 4-d$$

$$\gamma_{xy} = \frac{1}{G} \tau_{xy}; G = \frac{E}{2(1+\nu)} \quad 4-e$$

$$C = S^{-1} \quad 4-f$$

Where, 'C' is called the stiffness matrix.

Table 3-4 SiC properties derived after Post-processing MDS data.

<b>Silicon Carbide (SiC)</b>				
	300 K	800 K	1300 K	1800 K
Young's Modulus, E (GPa)	447.611	490.182	473.413	438.528
Poison's ratio, $\nu$	0.2313	0.2399	0.2287	0.2461
$C_{11}$ , (GPa)	520.045	580.632	572.793	530.881
$C_{12}$ , (GPa)	156.535	183.279	169.876	170.763

The above table 3-4 shows a significant increase in Young's modulus at 800 K and a gradual decrease as the temperature increases further. While calculating the Young's modulus we assume the SiC crystal to follow isotropic behavior. The results at 300 K are close to the reported values in table 4-1 and 4-2. The data does not show much deviation in the Poisson's ratio with variation in temperature indicating consistent material behavior along the longitudinal direction which is associated with the periodic boundary condition of the system.

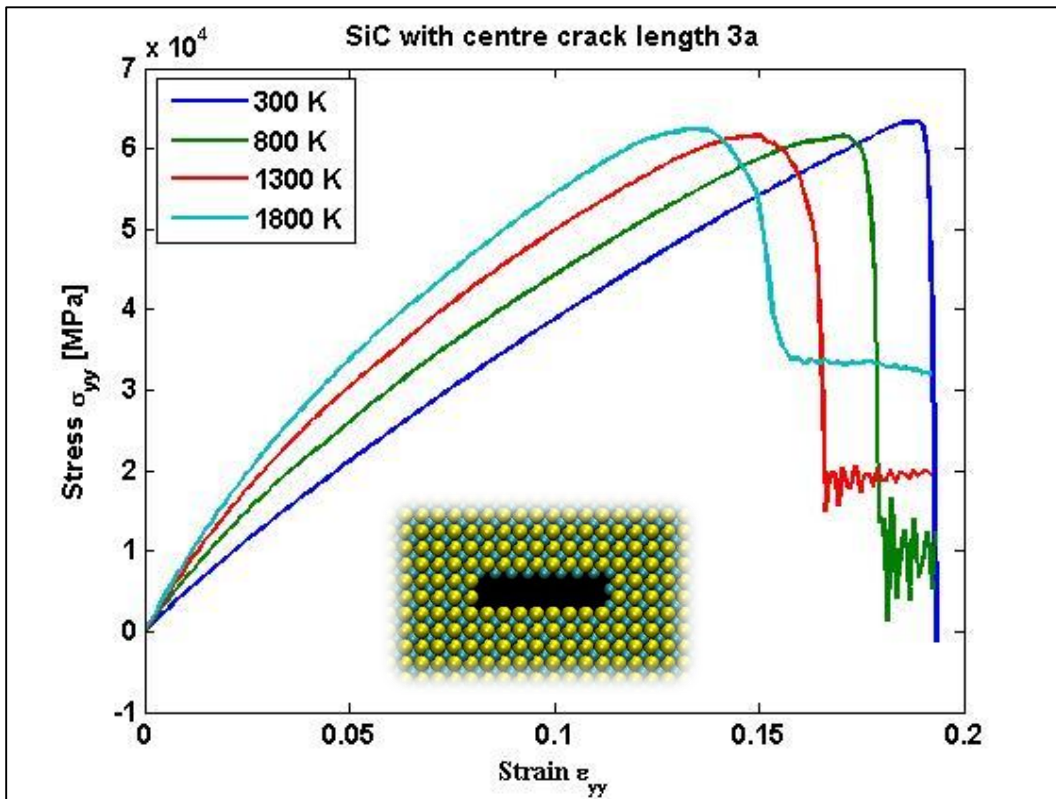


Figure 3-7 Plot of Stress vs. Strain for SiC w/ center crack = 3a.

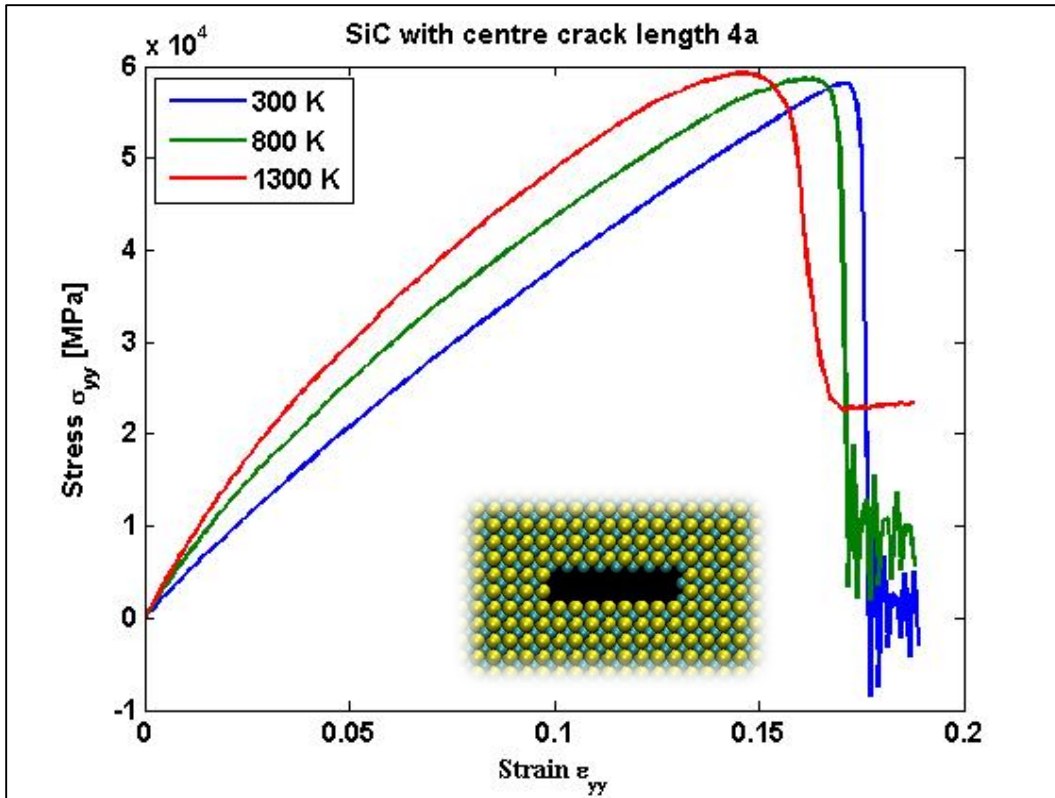


Figure 3-8 Plot of Stress vs. Strain for SiC w/ center crack = 4a.

From Fig: 4-7 and 4-8 we can see that as the temperature increases the ultimate tensile stress in y-direction remains almost constant whereas the strain reduces more significantly in comparison. The trend is consistent as the crack length is increased from 13.08 Å to 17.4 Å. As the temperature increases the peak reduces its sharpness indicating increase in elongation before failure. The increase in ultimate tensile stress can be associated to the fact that the material softens slightly at high temperatures. Also, the crack tip allows more deformation with the rise in temperature we see an increase in fracture toughness.

## Chapter 4

### Fracture Behavior of Hafnium Diboride (HfB<sub>2</sub>) Nano-Film

#### Overview

Ceramic borides, carbides also referred to as Ultra High Temperature Ceramics (UHTC) are materials notable for their high melting point, chemical inertness oxidation resistance and good compressive strength. They are considered in a wide range of applications such as cutting tools, reinforcement of metals, coating materials, catalyst and so on. Hafnium Diboride (HfB<sub>2</sub>) is one such material which is considered as a high temperature material for leading edges of hypersonic vehicles and for Thermal Protection System (TPS) of re-entry vehicles. But, most structural ceramics including HfB<sub>2</sub> are brittle and sensitive to cracks, pores and other superficial defects. Thus preventing wide usage due to concerns of unexpected failure which could lead to catastrophic results.

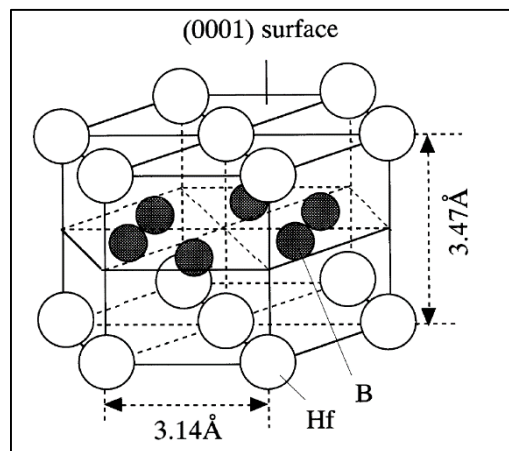


Figure 4-1 HfB<sub>2</sub> crystal structure. (Wataru Hayami, 1998)

Studies on such materials are in progress since the 1960's, still innovations in these material are required for stable, reliable and safe operation. To achieve this, better understanding of the effects of microstructure is needed. Until recent times computational modelling of such materials was limited due to absence of reliable inter-atomic potential

data. This chapter will study the effects of temperature on HfB<sub>2</sub> with various center crack lengths using Molecular Dynamics Simulations (MDS). Hafnium Diboride has a hexagonal crystal structure, with a molecular weight of 200.112 and melting point of ~3380°C.

Table 4-1 Properties of HfB<sub>2</sub>.

	C11	C13	C12	C33	C44
<i>Source [A]</i>	583.3	98.4	131.8	456.2	257.7
<i>Source [B]</i>	594	88	136	444	252

Table 4-2 Tersoff potential data for Hf and B atoms (Murray S. Dawa, 2011).

<b>Parameter</b>	<b>B</b>	<b>He</b>
A [eV]	1.0619848x10 <sup>3</sup>	3.15839x10 <sup>3</sup>
B [eV]	3.6767392x10 <sup>1</sup>	3.96250x10 <sup>2</sup>
$\lambda$ [Å <sup>-1</sup> ]	3.955278	2.83165
$\mu$ [Å <sup>-1</sup> ]	1.190167	0.65895
$\beta$	0.541	1
$\eta$	21.885575	1
c	0	0
d	1	1
h	0	0

Table 4-2 - continued

R [Å]	2.2	4.6
S [Å]	2.5	5
<b>Combination</b>	<b><math>\epsilon</math> [eV]</b>	<b><math>\sigma</math> [Å]</b>
Si-C	3.18	3.54

Table 4-2 is the Tersoff Potential data that will be as input in the field file used for simulation of HfB<sub>2</sub> molecular dynamics simulation tests.

#### HfB<sub>2</sub> Simulation Models:

Lattice constant:

$$a = 3.14 \text{ \AA}$$

$$c = 3.47 \text{ \AA};$$

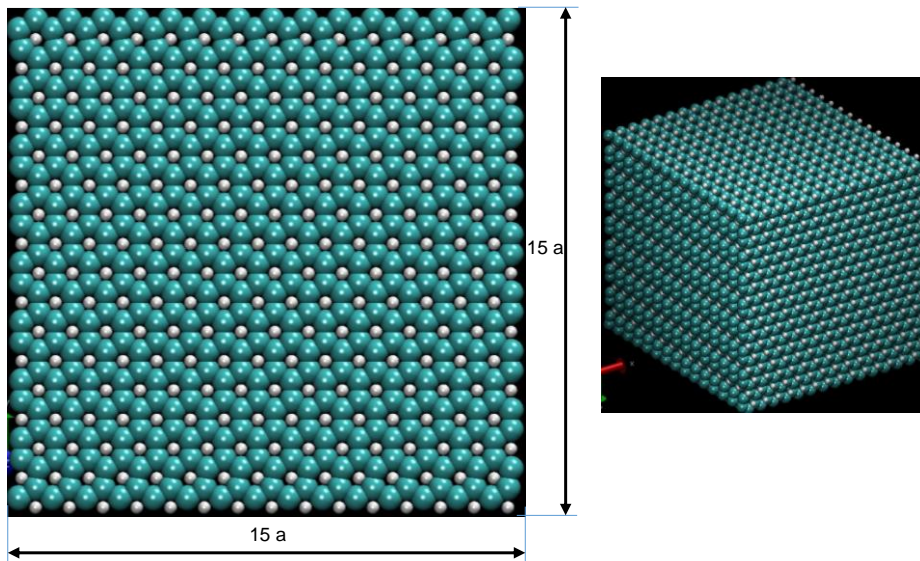


Figure 4-2 HfB<sub>2</sub> model using DL\_POLY GUI.

To carry out tensile HfB<sub>2</sub> models were developed as shown in figure 4-2. Models with center crack lengths 6.28Å and 9.42Å were also tested to obtain fracture properties of the material. The results obtained are tabulated in table 4-3.

### Results

#### *Effect of Temperature on Behavior of HfB<sub>2</sub>*

Table 4-3 HfB<sub>2</sub> properties derived after Post-processing MDS data.

<b>Hafnium Diboride (HfB<sub>2</sub>)</b>				
	300 K	800 K	1300 K	1800 K
Young's Modulus, E (GPa)	500.652	552.160	568.601	570.293
Poisson's ratio, $\nu$	0.3175	0.3299	0.3195	0.3239
C <sub>11</sub> , (GPa)	700.629	817.832	812.326	819.753
C <sub>12</sub> , (GPa)	330.568	402.645	381.406	407.648

The elastic properties of HfB<sub>2</sub> increase with increasing temperature as shown in the table above. The properties obtained from the literature at 300K shown in table 5-1 are less compared to the results obtained for 300K in table 5-3. This is due the difference in parameters used for test conditions and potential functions employed for the results in the literature. That said the results derived are consistent and are within range for atomistic data.

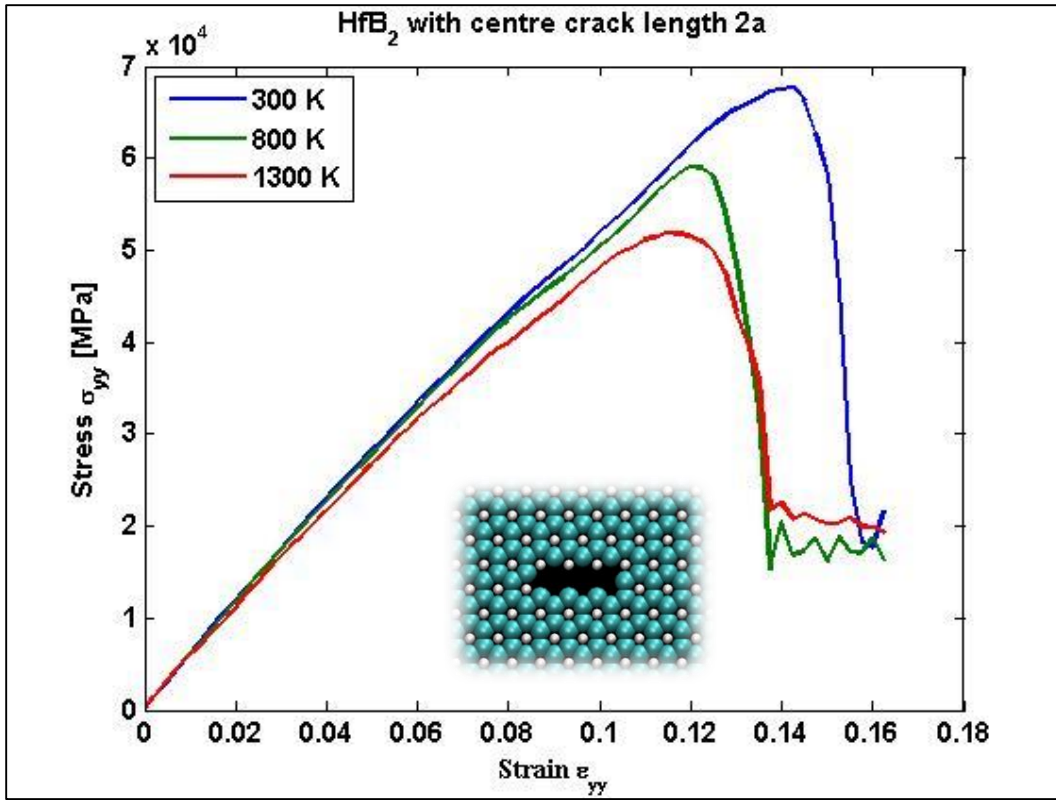


Figure 4-3 Plot of Stress vs. Strain for HfB<sub>2</sub> w/ center crack = 2a.



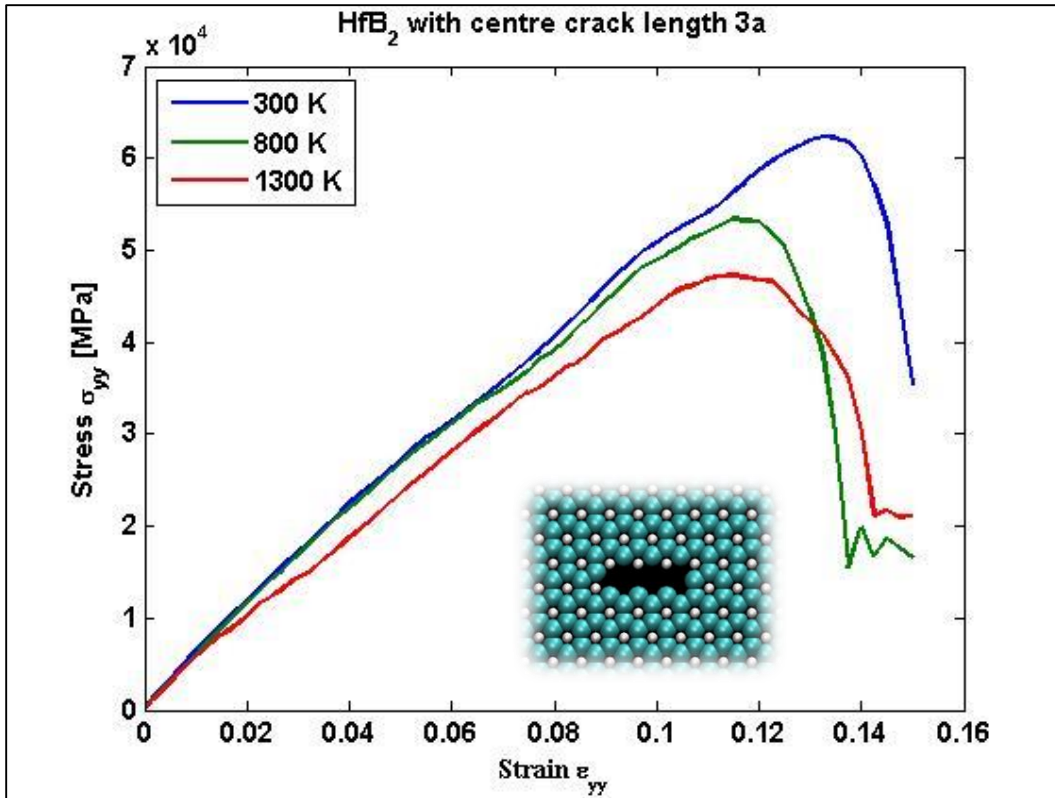


Figure 4-4 Plot of Stress vs. Strain for HfB<sub>2</sub> w/ center crack = 3a.

The Stress and strain graphs in figure 4-3 and 4-4 for HfB<sub>2</sub> with center crack length show similar trends at high temperatures to that of SiC. The sharp peak at room temperature is replaced by a gradual curve at higher temperatures indicating relatively less brittle fracture. At high temperatures the material softens slightly which allows additional elongation near the crack tip region in turn resulting in higher fracture toughness.

## Chapter 5

### Fracture Behavior of Layered Multi-Phase Composite Nano-Film

A multi-phase material can be described as one which is formed by a combination of different composition and are bonded together to retain their properties (Brook, 1986). An interface will exist in such materials which in turn will provide improved specific or synergistic characteristics previously not obtainable by each individual element. The objective of this research was to combine the two materials SiC and HfB<sub>2</sub> discussed above and analyze their behavior against their individual properties. The effects of high temperature on the composite form will result in the material behaving differently from that of the individual form which will play a key role in the application of it in Thermal Protection System.

For the purpose of this study SiC is considered as a layer over HfB<sub>2</sub>, the figure 5-1 below illustrates the models prepared to calculate the properties at high temperature.

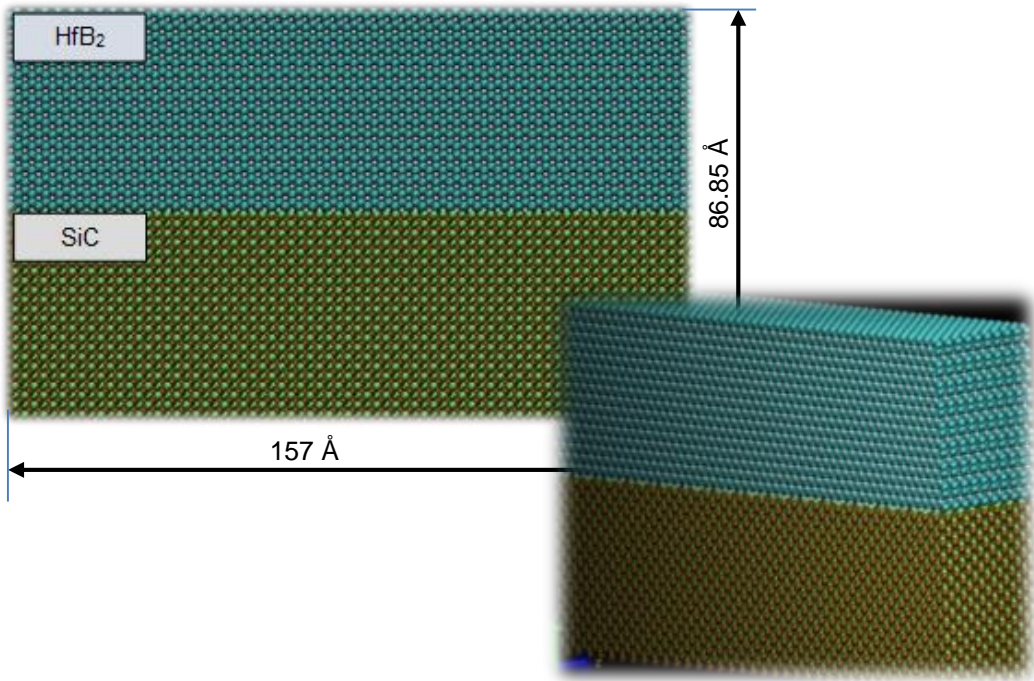


Figure 5-1 Layered nano-film model.

## Results

### *Multiphase Properties of Layered Nano-Film*

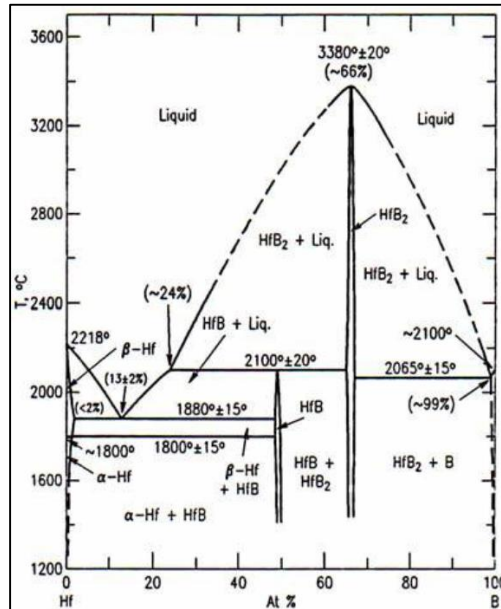


Figure 5-2 Phase Diagram of Hf - B

The melting temperature for HfB<sub>2</sub> is 3653 K (J.F. Justin, November 2011) and that of SiC is 3003 K (Abbaschian, 1984). To find the melting point of the layered Nano-film, a simulation was done by increasing the temperature of the system to 5000K. From the Energy and Temperature data with respect to time a graph for Energy vs. Temperature is plotted. Point 'c' denotes the change in phase of the material from solid to liquid, line 'b' is the solid phase, line 'a' is the liquid phase and difference between the points 'c' and 'd' is the 'Latent Heat of Absorption' (Lock, 1996).

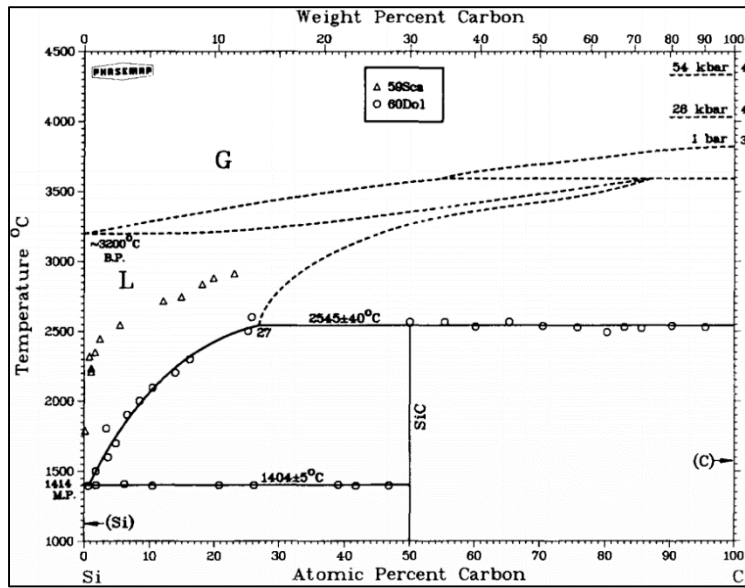


Figure 5-3 Phase diagram for Si - C

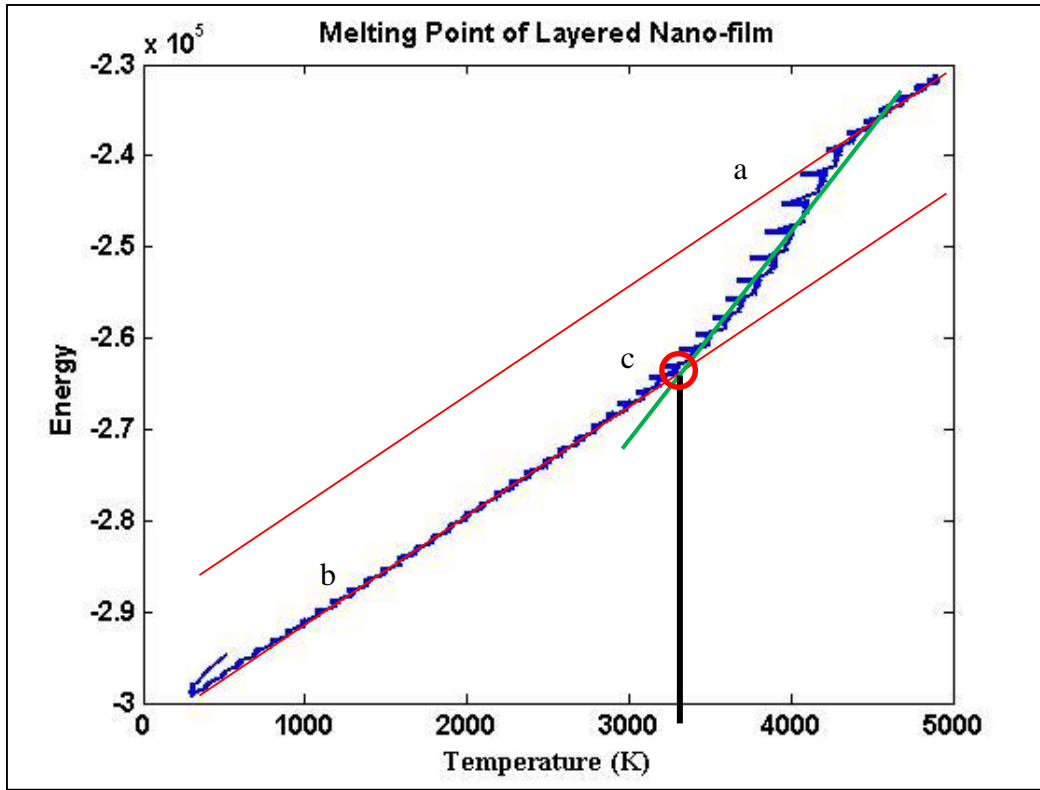


Figure 5-4 Energy vs. Temperature plot for Layered Nano-film.

*Effect of Temperature on Behavior of Layered  $\text{HfB}_2\text{-SiC}$  Nano-film*

The Tersoff potentials in table 3-3 and 4-2 are used together in the FIELD file for running simulations for the layered nano-film models. Figure 5-1 shows the layered nano-film model which contains a total of 50844 atoms and is tested without crack and later with a center crack of  $12.42\text{\AA}$

Table 5-1 Layered HfB<sub>2</sub>-SiC properties derived after Post-processing MDS data.

<b>Layered HfB<sub>2</sub> – SiC Nano-film</b>				
	300 K	800 K	1300 K	1800 K
Young's Modulus, E (GPa)	576.453	630.697	593.896	618.033
Poisson's ratio, $\nu$	0.3172	0.3019	0.2996	0.3188
C <sub>11</sub> , (GPa)	817.421	853.800	798.707	821.521
C <sub>12</sub> , (GPa)	379.796	369.389	341.742	359.613

The results clearly show good performance in elastic properties at high temperature for the layered Nano-film composite. An increasing trend in the Young's modulus is observed with increasing temperature and a consistent value of Poisson's ratio. Although there is a drastic increase in elastic properties from room temperature to 800K this can be associated with the isotropic assumptions considered for simplifying the calculations.

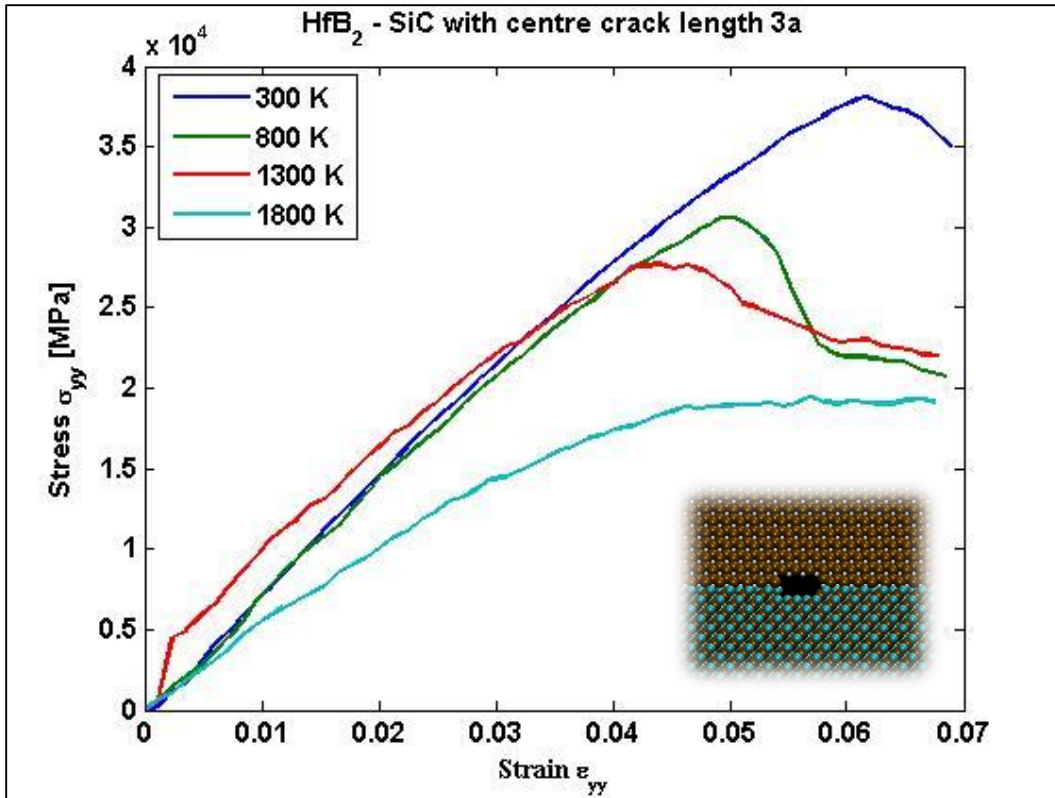


Figure 5-5 Plot of Stress vs. Strain for HfB<sub>2</sub> - SiC w/ center crack = 3a.

The above graph confirms that the earlier predictions for the layered Nano-film to show increase in strain to failure ratio is true. At 1800K the material shows higher strain as compared to room temperature which is desirable. The material shows relative ductility at higher temperatures when compared to pure HfB<sub>2</sub> and SiC and also at room temperature for layered Nano-film.



## Chapter 6

### Conclusion

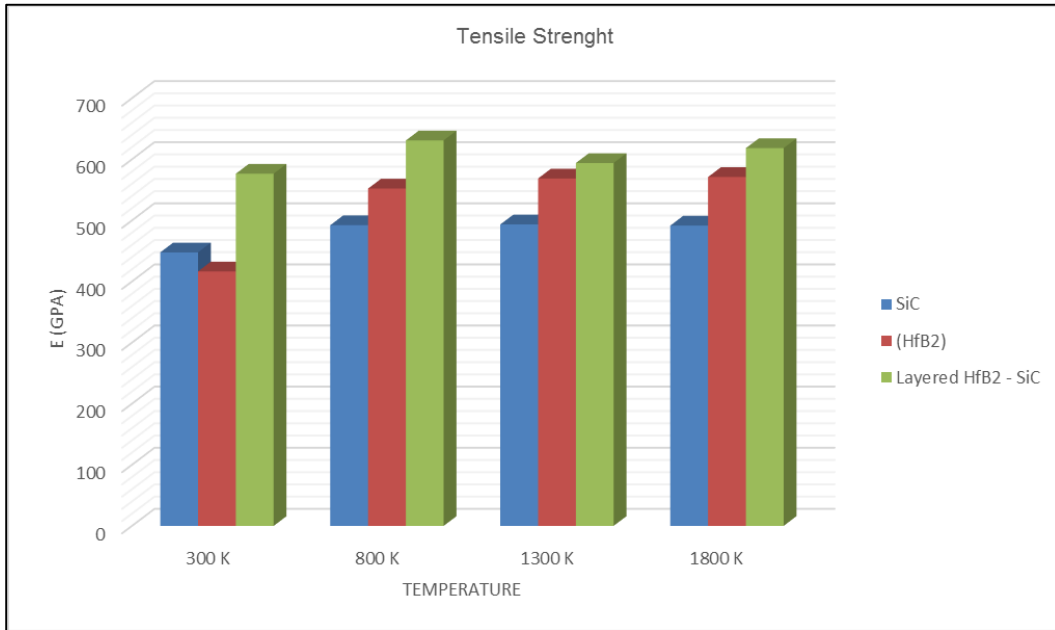


Figure 6-1 Comparison of Layered HfB<sub>2</sub>-SiC tensile strength to individual elements.

The figure above illustrates the comparison between Young's modulus of individual elements, HfB<sub>2</sub> and SiC vs. layered nano-film of the composite. It clearly indicates an improvement to the elastic properties at room temperature as well as higher temperatures.

From Table 8-1 we can see the improvement in elastic properties for the layered nano-film of the composite over pure SiC material is in the range of 20-30% from room temperature to 1800K, this is a significant improvement which was predicted at the beginning of this study. There is a similar trend in improvement of elastic properties for HfB<sub>2</sub> ranging from 5-15%.

Table 6-1 Tensile strength improvement in layered HfB<sub>2</sub>-SiC

Layered HfB <sub>2</sub> - SiC	300 K	800 K	1300 K	1800 K
% Improvement from Pure SiC	28.78	28.19	20.36	25.79
% Improvement from Pure HfB <sub>2</sub>	18.80	14.26	4.45	8.26

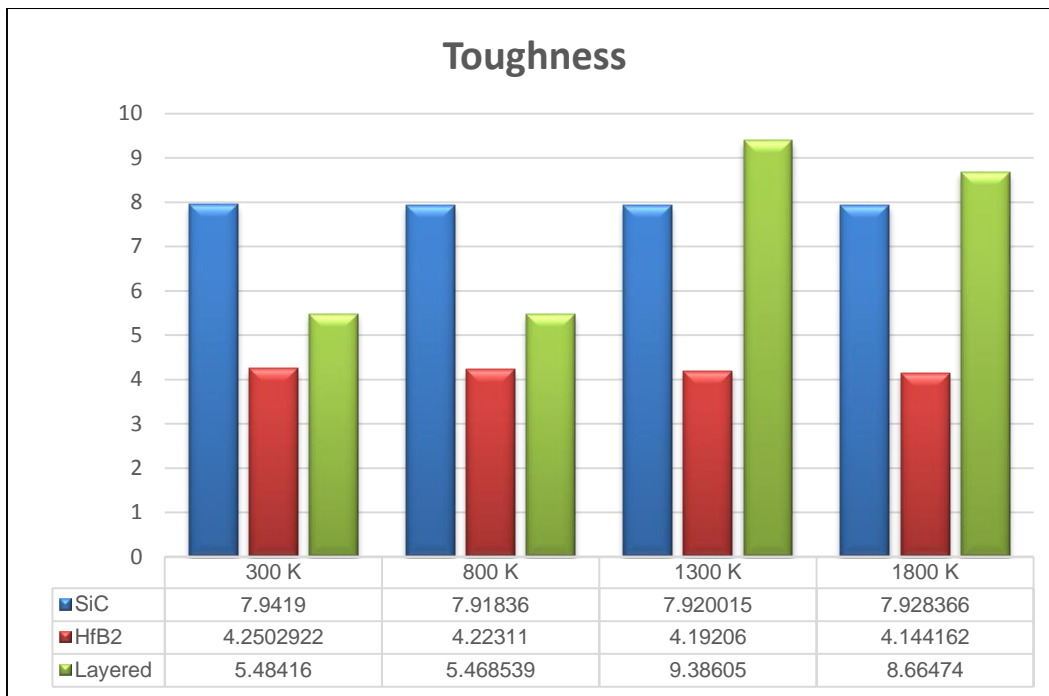


Figure 6-2 Comparison of Layered HfB<sub>2</sub>-SiC toughness to individual elements.

From Table 6-2 the toughness of layered Nano-film shows improvement from pure HfB<sub>2</sub> at room temperature and through high temperatures. Whereas compared to pure SiC there is no improvement, in fact the toughness decreases for the layered Nano-film at room temperature. There is significant improvement in toughness for the layered Nano-film at 1300K and 1800K. This can be explained by the formation of boro-silicate (Carney, 2009) glass at the interface of the two materials which results in increased toughness.

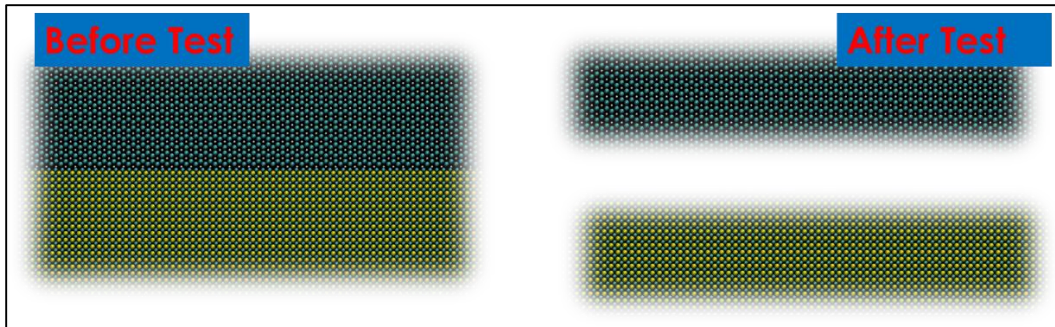


Figure 6-3 Illustration of layered HfB<sub>2</sub>-SiC failure.

Figure 6-3 shows that the failure in layered Nano-film occurs at the interface and is along the longitudinal axis. As a future scope of study this region of weakness can be further strengthened by varying the interface geometry. Below are a few suggestions for improvement;

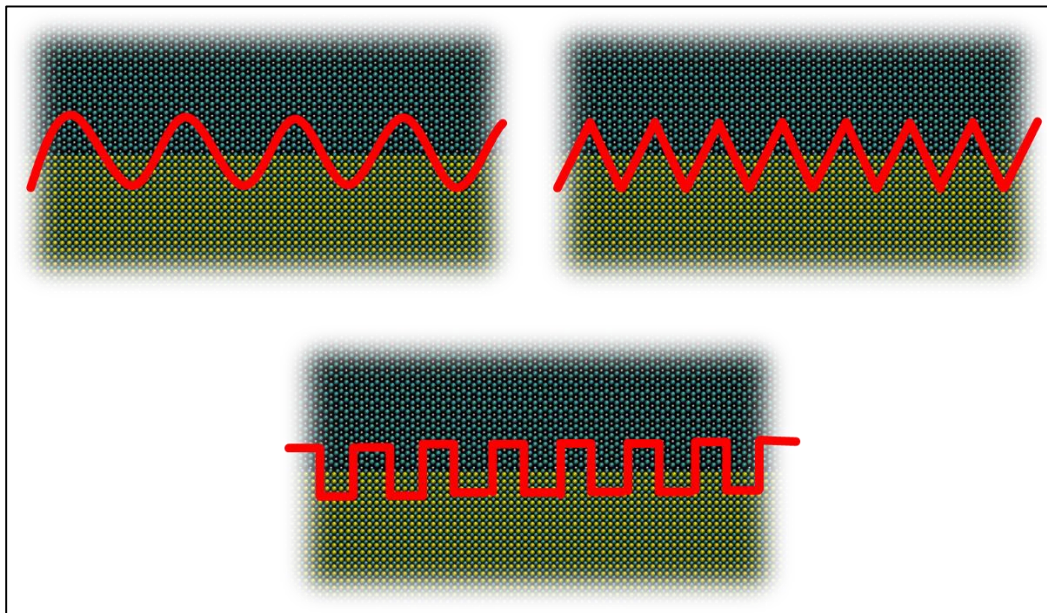


Figure 6-4 Suggested improvements at the interface to further improve toughness.

The suggestions in figure 6-4 are based on two intuitive reasons:

- i. Increasing the surface area for the interface will increase the energy required to create new surfaces

ii. Uneven geometry will result in deflecting the failure path of the material.

Thus requiring additional energy to traverse a different path.

Also, in reality manufacturing a smooth surface without irregularities is very difficult.

Studying further for irregular interface geometries will give a better outlook on the fracture properties for this system

## Bibliography

1. "Elevated Temperature Thermal Properties of ZrB<sub>2</sub> with Carbon Additions" November 30, 2011 *Journal of the American Ceramic Society*
2. "Mechanical Characterization of ZrB<sub>2</sub>-SiC Composites with Varying SiC Particle Sizes," 2011 *Journal of the American Ceramic Society*
3. 2004 *Materials Science and Engineering*
4. August 2005 *Atomistic Calculations of Nanoscale Interface Behavior in FCC Metals* Georgia Institute of Technology
5. Basics of Molecular Dynamics Romania Babeş-Bolyai University
6. Computational design of novel carbon enriched Si<sub>1-x</sub>C<sub>x</sub> ceramics: A molecular dynamics simulation study January 2015 *Computational Materials Science* Pages 354-359
7. Continuum interpretation of virial stress in molecular simulations July 2008 *International Journal of Solids and Structures* Volume 45, Issues 14–15, Pages 4340-4346
8. Crack-healing behavior of zirconium diboride composite reinforced with silicon carbide whiskers 15 August 2008 *Center for Composite Materials, Harbin Institute of Technology*
9. DL\_POLY 2006 *Journal of Materials Chemistry*
10. *Fundamentals of metal fatigue analysis* 1989 New Jersey Prentice Hall
11. General Properties of Bulk SiC 2014 Springer
12. Improving Fracture Toughness of Silicon Carbide Ceramics with Nanodiamond Reinforcements 2013 American Society for Composites
13. Interatomic potentials for Zirconium Diboride and Hafnium Diboride 2011 *Computational Materials Science*

14. 2001 *Introduction to Fracture Mechanics* Cambridge, MA Massachusetts Institute of Technology
15. *Latent Heat Transfer: An Introduction to Fundamentals* 1996 Pennsylvania State University Oxford University Press
16. *Lattice thermal conductivity of ultra high temperature ceramics ZrB<sub>2</sub> and HfB<sub>2</sub> from atomistic simulations* NASA Ames Research Center and Clemson University
17. Marine-Based Carbon and Silicon Carbide Scaffolds with Patterned Surface for Tissue Engineering Applications 2011 *Advances in Ceramics*
18. Microtek Laboratories *Fracture Toughness: Critical stress-Resistance-Testing* Anaheim, CA
19. Molecular Dynamics Simulation of Nanoindentation on Ion-induced Damage of Silicon Surface 2009 *Journal of Physics*
20. 2005 *Molecular Dynamics Studies of the Fracture of Metals* Yeshiva university
21. Oxidation resistance of hafnium diboride—silicon carbide from 1400 to 2000 degC 2009 *Journal of Material Science*
22. Role of nanoparticle dispersion and filler-matrix interface on the matrix dominated failure of rigid C 60-PE nanocomposites: A molecular dynamics simulation study 2013 *Polyme*
23. Roylance, D. (2000). *Laminated Composite Plates*. Cambridge: Department of Materials Science and Engineering, Massachusetts Institute of Technology.
24. *Sintering of Multi-phase Ceramics* 1986 Plenum Press
25. Stability of metal ions in molten glass: the definition of reduction and oxidation April 1999 *Physics and Chemistry of Glasses*, Volume 40, Page 54-56(3)
26. Structural analysis of the HfB<sub>2</sub> surface by impact-collision ion scattering spectroscopy 1998 *Surface Science*

27. Temperature Jump Phenomenon During Plasmatron Testing of ZrB<sub>2</sub>-SiC Ultra-High Temperature Ceramics 2011 *Journal of Thermophysics and Heat Transfer*
28. The C-Si (Carbon-Silicon) System 1984 *Bulletin of Alloy Phase Diagrams*
29. The Effects of Filler-Matrix Interface Strength, Filler Shape And Filler Dispersion On The Mechanical Properties of Polymer Nanocomposites 2012 American Society for Composites
30. August 3, 2011 *Ultra High Temperature Ceramics: Application, Issues and Prospects* Baltimore, MD NASA-Ames Research Center
31. Ultra High Temperature Ceramics: Densification, Properties and Thermal Stability November 2011 *Aerospace Lab*
32. W. Smith, T. F. (2009). *The DL\_POLY Usermanual*. Chesire, UK: STFC Daresbury Laboratory.

### Biographical Information

Zoher Shabbir Lavangia was born October 7<sup>th</sup>, 1991 Bombay, India. He earned his Diploma in Mechanical Engineering from M. H. Saboo Siddik Polytechnic, Mumbai, India and received his Bachelors of Engineering in Aeronautical Engineering from Hindustan University, Chennai, India. He has also completed a certification course in 3D modelling and analysis from CADD centre. In fall 2013 he joined the Masters of Science program in Aerospace Engineering at The University of Texas at Arlington.

While pursuing his Masters, Zoher carried out research in the field of Nano-Composites in the Multi-scale Mechanics and Physics Lab under the guidance of Dr. Adnan Ashfaq. During this period he presented his work on High Temperature Nano-Composites at ACES (Annual Celebration of Excellence by Students) UTA, 2015 and was a co-author for a paper submitted at IMECE(International Mechanical Engineering Conference and Exposition), ASME 2015. Zoher has also worked on several other projects namely; Design analysis of Space Transportation System (Space Shuttle), Design and fabrication of Scaled– down model of an EAGLE etc.

Apart from his academic career Zoher like to Travel to new destinations and involve in outdoor adventure sports. He also enjoys cooking and trying new cuisines. He also likes to swim, play badminton, table tennis and other outdoor sports.

Zoher plans to pursue a career in commercial aviation industry and contribute his innovative ideas to benefit the world community.